Phased Array Satellite Antenna Testing by an Aircraft Borne Emulation Platform

Iwan Kruger
Dept. of Electrical and Electronic Engineering
Stellenbosch University
Stellenbosch, South Africa
iwankruger@gmail.com

Riaan Wolhuter
Dept. of Electrical and Electronic Engineering
Stellenbosch University
Stellenbosch, South Africa
wolhuter@sun.ac.za

***Abstract*—The KU Leuven- and Stellenbosch Universities are jointly developing an electronically beam steerable phased antenna array for satellite applications, including all the peripheral ground- and space segment subsystems. This paper covers the development of an Aircraft based Satellite Emulator to facilitate convenient aircraft based testing of an antenna array, intended for Low Earth Orbit satellite deployment. A flight strategy is developed to emulate such a satellite as best possible, with the strategy subsequently implemented in software on in-flight PC hardware. The emulator acts as a full interface between the aircraft avionics and satellite bus system, to enable generation of the required antenna steering commands and to create a satellite bus image to the payload. The emulator provides in-flight systems information to the satellite payload, as it would get from an actual satellite bus during spaceflight. The emulator ensures indifference to the payload, regardless of the fact that testing is aircraft based. An embedded control algorithm for the steerable antenna has also been developed and resides in the onboard computer of the payload. Excellent initial test results have been obtained from the aircraft flight simulator and actual flight telemetry data, proving the viability and cost-effectiveness of the approach. The system tests as reported on here, stopped just short of full equipment flight testing, as scheduled for in the near future. This is awaited with keen interest, as all results up to the present have been positive and in line with expectations.**

***Index Terms*—Satellite Emulator; Phase Array Antenna; Beam Steering; Orbital Calculations; Link Budgets;**

I. Introduction

The feasibility of utilising electronically beam steerable antenna arrays (SAA) in space, is currently jointly being investigated by the ESAT-TELEMIC division of the Department of Electrical Engineering, Katholieke Universiteit Leuven, (KUL) Flanders, in partnership with the Department of Electrical and Electronic Engineering, Stellenbosch University, South Africa. Successful space implementation of such an antenna array promises a number of significant benefits and the development of advanced techniques therefor, has been the subject of our joint research and development for some time [1], [2]. Amongst others, it will reduce the cost of ground stations by eliminating tracking antennas and reducing RF chain complexity, while still retaining an acceptable link budget. By introducing beam steered satellite antenna tracking of ground stations during overflight, the link budget could be improved and ground station complexity reduced, particularly with regard to antenna design and the RF chain. These ground nodes are typically used for environmental and agricultural data acquisition and any improvement regarding the above are always beneficial. The Stellenbosch University member of this partnership, is responsible for development of the satellite platform hosting the SAA, ground station and accompanying ground-space communications link. The payload would be deployed on a next South African low earth orbit (LEO) satellite. Development and construction of any form of space borne system is normally expensive and associated with many risks. It was, therefore, decided to introduce an interim testing phase prior to actual space flight, by using a light aircraft as a pseudosatellite test platform. This will offer the obvious advantages of convenient and relatively cheap closed loop system testing and debugging. This must, without doubt, enhance the chances of eventual in-flight success. The aircraft itself has been fitted out for experimental use and will house the SAA, the entire satellite payload containing the On Board Computer (OBC), communications link component chain, steerable antenna control/status interface, power supplies, as well as an Aircraft Satellite Emulator (ASE). In actual deployment, all interaction with the rest of the satellite is via a system bus for purposes of telecommand, telemetry and attitude/positioning information. The ASE is obviously required to act as translator and emulator between the payload and aircraft, the latter acting as pseudo-satellite. As far as the payload is concerned, it should behave as if connected to the actual satellite bus. The ASE and developed emulation strategy can be adapted to various LEO satellite payloads and thus provides a general low cost test platform prior to space deployment. The purpose of this paper is to report on the development of the emulation platform and SAA control subsystems. Some very encouraging results have been presented elsewhere [1], which have since been confirmed and expanded by continued pre-flight testing. The paper will describe the required flight path mechanics, the feasibility of an emulation strategy, a brief description of the implementation and test results obtained from an aircraft simulator and aircraft flight telemetry data. The rest of the paper is structured as follows: An overview of the relevant orbital mechanics in Section II, is followed by the discussion of the required emulation strategy in Section III. Calculation of the aircraft flight path parameters in order to satisfy the emulation strategy, is covered in Section IV. These basic

operational requirements are then utilised for the systems design as set out in Section V. Evaluation and test results were obtained from simulations, a flight simulator and actual flight telemetry data. These are presented in Section VI. Section VII contains a summary of the work performed, results obtained and a view of the way forward.

II. Orbital Calculations

Before discussing the emulation strategy as developed, it might be useful to present a brief refresher on satellite orbital mechanics, as these are fundamental to the system design. The calculations presented in this section are based on a spherical earth model, which is adequate for this particular type of application [3]. The oblateness of the earth and the varying topography on the surface, are treated as coordinates above or below the spherical surface of the earth.

A. Angular velocity

The angular velocity of a satellite in orbit can be calculated by:

$$\omega = \sqrt{\frac{GM_E}{r^3}} \qquad (s^{-1}) \tag{1}$$

where r (m) is the circular orbit radius, the universal gravitation constant $G = 6.672 \times 10^{-11}\,\mathrm{m^3 kg^{-1} s^{-2}}$, and the earth mass $M_E = 5.974 \times 10^{24}\,\mathrm{kg}$[4].

B. Coordinates

The locations of the satellite and ground stations are specified in latitude, longitude and radius coordinates, and can be expressed in celestial coordinates originating at the earth's centre, as per Figure 1.

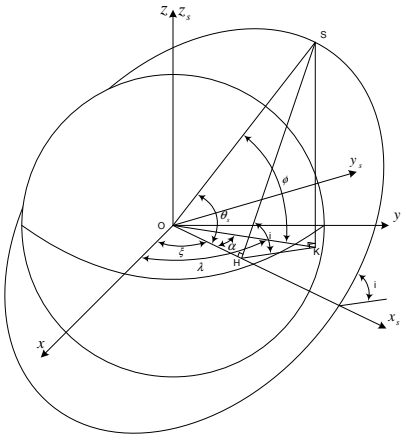

Fig. 1. Celestial coordinate structure

1) Satellite coordinates: The satellite position is first described by the (x_s, y_s, z_s) coordinate system (Figure 1). The x-axis is directed to the intersection of the satellite orbital path and the equatorial plane. The satellite coordinates in this coordinate frame are:

$$x_s = R\cos(\theta_s) \tag{2}$$
$$y_s = R\sin(\theta_s)\cos(i) \tag{3}$$
$$z_s = R\sin(\theta_s)\sin(i) \tag{4}$$

where i is the inclination angle and $\theta_s = \theta_0 + (\omega_{sat})(t)$ the orbit angle. The initial orbit angle can be calculated by:

$$\theta_0 = \arcsin\left(\frac{\sin(\phi_0)}{sin(i)}\right) \tag{5}$$
$$\tag{6}$$

where ϕ_0 is the initial latitude coordinate of the satellite and ω_{sat} the angular velocity.

A transformation is required to describe the (x_s, y_s, z_s) coordinates in a celestial coordinate system. The transformation is presented in the following matrix notation:

$$\begin{bmatrix} x_{Sat} \\ y_{Sat} \\ z_{Sat} \end{bmatrix} = \begin{bmatrix} \cos(\xi) & \sin(\xi) & 0 \\ -\sin(\xi) & \cos(\xi) & 0 \\ 0 & 0 & 1 \end{bmatrix} \begin{bmatrix} x_s \\ y_s \\ z_s \end{bmatrix} \tag{7}$$

The ξ angle is obtained as $\xi = \alpha - \lambda_{Sat,0}$ where $\lambda_{Sat,0}$ is the initial longitude coordinate of the satellite. α can be calculated as:

$$\alpha = \arccos\left(\frac{\cos(\theta_0)}{cos(\phi_0)}\right) \tag{8}$$

Thus, the satellite coordinates are given by:

$$x_{Sat} = R\cos(\theta_s)\cos(\xi) + R\sin(\theta_s)\cos(i)\sin(\xi) \tag{9}$$
$$y_{Sat} = -R\cos(\theta_s)\sin(\xi) +$$
$$= R\sin(\theta_s)\cos(i)\cos(\xi) \tag{10}$$
$$z_{Sat} = R\sin(\theta_s)\sin(i) \tag{11}$$

2) Ground station coordinates: From Figure 1, the ground station coordinates transformed to the celestial coordinate system, are defined by:

$$x_{GS} = R_{GS}\cos(\phi_{GS})\cos(\lambda_{GS}) \tag{12}$$
$$y_{GS} = R_{GS}\cos(\phi_{GS})\sin(\lambda_{GS}) \tag{13}$$
$$z_{GS} = R_{GS}\sin(\phi_{GS}) \tag{14}$$

with $\lambda_{GS}(t) = \lambda_{GS,0} + (\omega_{GS})(t)$, where $\lambda_{GS,0}$ is the initial longitude coordinate of the ground station and ω_{GS} the angular velocity of the Earth. [5]

C. Distance to satellite

If the coordinates of the satellite and ground station are known, the varying distance D between the ground station and the satellite can be obtained quite simply by Pythagorean geometry.

$$D = \sqrt{(x_{Sat} - x_{GS})^2 + (y_{Sat} - y_{GS})^2 + (z_{Sat} - z_{GS})^2} \tag{15}$$

D. Geocentric angle

The geocentric angle (ψ) between the satellite nadir point and a ground station placed at the centre of the earth, can be determined by the cosine rule.

$$\psi = \arccos\left(\frac{R_{GS}^2 + R_{sat}^2 - D^2}{2 \cdot R_{GS} \cdot R_{sat}}\right) \quad (16)$$

E. Elevation angle

The elevation angle (E) is the angle between the horizon and the satellite.

$$E = \left| \arcsin\left(\frac{R_{sat}\sin(\psi)}{D}\right) - \frac{\pi}{2} \right| \quad (17)$$

F. Azimuth angle

The azimuth angle is the angle measured Eastward from North, to the nadir point at the ground station, as per angle NPT in Figure 2.

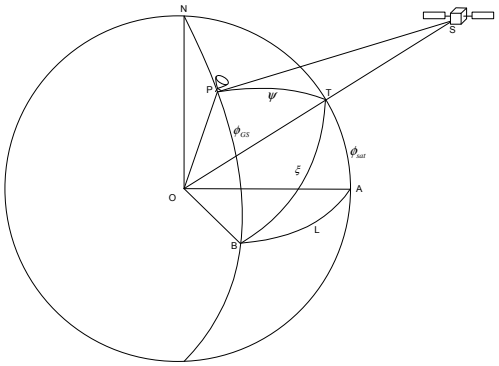

Fig. 2. Earth satellite geometry (reproduced from [6])

For the spherical triangle NPT of Figure 2:

$$\frac{\sin(NPT)}{\sin(90^\circ - \phi_{sat})} = \frac{\sin(NPT)}{\cos(\phi_{sat})} = \frac{\sin(PNT)}{sin(\psi)} \quad (18)$$

For the spherical triangle NBA the angle BAN and AON is equal to 90°, therefore

$$\frac{\sin(BNA)}{\sin(L)} = \frac{\sin(BAN)}{\sin(AON)} = 1 \quad (19)$$

Because angle BNA = PNT, equation 19 can be substituted into equation 18 with the result:

$$\sin(NPT) = \frac{\sin(L)\cos(\phi_{sat})}{\sin(\psi)} \quad (20)$$

$$a = NPT = \arcsin(\frac{\sin(L)\cos(\phi_{sat})}{\sin(\psi)}) \quad (21)$$

where ψ is the geocentric angle, ϕ_{sat} the latitude coordinate of the satellite and

$$L = |\lambda_{GS} - \lambda_{sat}| \quad (22)$$

the difference between the longitude coordinates of the ground station and the satellite. To obtain the true azimuth angle (A), we need to consider the position of the nadir, (point T in Figure 2) relative to the ground station (point P in Figure 2). The various cases can be summarised as follows:

$$A = \begin{cases} 180^\circ - a & \text{if } \lambda_{GS}(t) - \lambda_{sat}(t) > 0 \text{ and } \phi_{GS}(t) - \phi_{sat}(t) < 0 \\ a & \text{if } \lambda_{GS}(t) - \lambda_{sat}(t) > 0 \text{ and } \phi_{GS}(t) - \phi_{sat}(t) > 0 \\ 180^\circ + a & \text{if } \lambda_{GS}(t) - \lambda_{sat}(t) < 0 \text{ and } \phi_{GS}(t) - \phi_{sat}(t) < 0 \\ 360^\circ - a & \text{if } \lambda_{GS}(t) - \lambda_{sat}(t) < 0 \text{ and } \phi_{GS}(t) - \phi_{sat}(t) > 0 \end{cases} \quad (23)$$

G. Steering angles

This section will describe the basic strategy to calculate the ϕ (phi) and θ (theta) angles. These angles will enable the airborne object to track the specified ground station. The ϕ angle is measured from the positive x-axis of the body frame toward the positive y-axis, in the x-y plane. The θ angle is measured from the positive z-axis of the body frame, towards the position vector. Figure 3 defines the parameters used to calculate these angles.

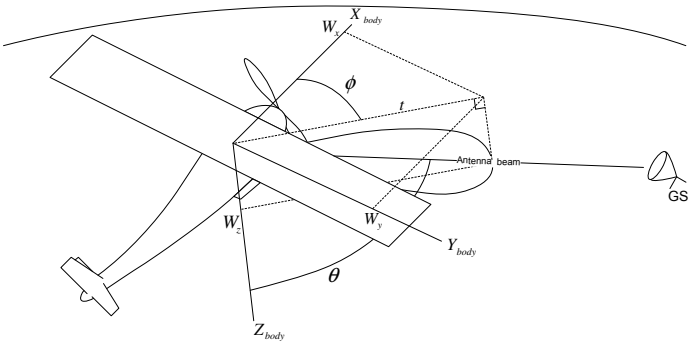

Fig. 3. Defining parameters used to calculate the θ and ϕ angles.

The coordinates (LLA), specified as latitude, longitude and altitude, are known for both the airborne object and ground station. The first step is to convert these coordinates from the LLA system to the ECEF frame, by making use of the World Geodetic System 1984 standard. (WGS-84)[7]. The results can be written as follows:

$$\vec{R}_{Sat} = \begin{bmatrix} X_{Sat} & Y_{Sat} & Z_{Sat} \end{bmatrix}^T and \quad (24)$$

$$\vec{R}_{GS} = \begin{bmatrix} X_{GS} & Y_{GS} & Z_{GS} \end{bmatrix}^T \quad (25)$$

The airborne object to ground station position vector is then calculated as

$$\vec{R}_{pos} = \vec{R}_{GS} - \vec{R}_{Sat} \quad (26)$$

The position vector can now be converted from the ECEF frame to the NED frame situated at the airborne object.

$$\vec{B} = \mathbf{K} \cdot \vec{R}_{pos} \quad (27)$$

where $\mathbf{K}$ is the transformation matrix [8].

It is necessary to take the attitude of the object into account by describing the object in terms of its pitch, roll and yaw Euler angles. By using an Euler 123 rotation [9] to transform the position vector from the NED frame to the body frame of the object, it is possible to describe the position vector from the

object to the ground station in terms of the orientation of the object. The θ and ϕ angles can be calculated after accounting for the attitude of the object.

$$\vec{W} = \mathbf{A} \cdot \vec{B} \tag{28}$$

The θ and ϕ angles are relative to the body frame of the object. These angles direct the position vector to the target or ground station and can be calculated by means of simple trigonometry.

The theta θ angle is calculated as:

$$t = \sqrt{W_x^2 + W_y^2} \tag{29}$$

$$\theta = \frac{\pi}{2} - \arctan\left(\frac{W_z}{t}\right) \tag{30}$$

$$= \frac{\pi}{2} - \arctan\left(\frac{W_z}{\sqrt{W_x^2 + W_y^2}}\right) \tag{31}$$

The ϕ angle is calculated as:

$$\phi = \arctan\left(\frac{W_y}{W_x}\right) \tag{32}$$

III. Emulation Strategy

This section presents a few emulation strategies as considered and the reasons for selecting a particular one.

Two main emulation approaches were considered. The first approach was to emulate the satellite position relative to a ground station and the second to emulate the ground station position relative to a satellite. It is clear that for the first case the position could be described by elevation and azimuth angles [10]. The second approach describes the position of a ground station from the perspective of a satellite using the ϕ and θ angles. These angles are, in both cases, time dependent for LEO satellites. The function of the emulator is to calculate a flight route for an aircraft that would approximate these orbital characteristics as closely as possible.

A. Flight Strategy

1) The first emulation flight strategy considered was to fly in ascending concentric circles around a ground station. This strategy covers all the azimuth and ϕ angles for a specific elevation or θ angle. By spiralling upwards it is possible to cover many elevation and θ angles. The implementation of this strategy is however arduous. It is difficult for an aircraft to fly at a constant speed in an accurate, circular, upwards path around a ground station. However, the main disadvantage of this option is that the specific time variant behaviour of practical elevation-azimuth and ϕ-θ angles are not taken into account.
2) The second strategy entailed flying past a ground station in a straight path parallel to the earth surface at a constant speed and altitude. It is easier for a pilot to implement this strategy than the previous one and he will be able to maintain a more stable attitude. Because of this and with the aircraft flying parallel to the surface, the orientation of the antenna on the aircraft will match the predicted orientation of the antenna on the satellite more closely. The orientation of the antenna will enable the steering angles of the antenna to approach that of the actual satellite implementation, providing a more realistic scenario. The orientation will also facilitate the calculation of a more accurate linkbudget for a flight path. The linkbudget can then be emulated by compensating for the L_{FS} losses by attenuating the transmitting or receiving signal. The further advantage of this strategy is that the specific time variant behaviour of the elevation-azimuth and ϕ-θ angles of a LEO satellite are taken into account. This will also enable the relationship between the antenna steering angles and time to match that of the satellite application. For these reasons the second strategy is clearly the better one and was selected for actual implementation.

B. Transmission Link Strategy

With the aircraft based flight test, the direct LOS distance to a ground station is clearly much shorter than in the case of a real satellite. In order to emulate the satellite link budget, the free space loss (FSL) must be compensated for. The calculated FSL is shown in Figure 20. The aircraft link must, therefore, be attenuated to achieve the FSL of a satellite link. This could be simply done by adjustment of the transmit power for both the up- and down links.

Doppler shift is not a consideration for the aircraft flight test due to the low speed, but certainly affects the satellite link. The amount of required compensation will be determined by final orbit and receiver front-end selectivity bandwidth. For this project, Doppler compensation will probably be performed at the ground station and therefore, no compensation has been implemented on the emulator platform.

To minimise the affect of terrain scattering, the emulation flight tests are planned for a wide open semi-desert area.

Table I shows the losses caused by the distance between the ground station and the aircraft at various maximum elevation angles. Losses between the ground station and the satellite is displayed in the last column of Table I. The amount of attenuation can thus be calculated by subtracting the satellite free space losses from those of the aircraft at a specific altitude and maximum elevation angle.

IV. Calculation of Aircraft Parameters

In order to implement the chosen strategy as discussed in the previous section, it is necessary that the aircraft flight parameters be calculated in terms of the required trajectory. This calculation was done by means of a suitable script, based on the elevation-azimuth approach, as explained in Section III.

The script is fed with the maximum elevation angle as an input parameter. The maximum elevation angle occurs when the object is closest to the ground station. The script then calculates the time values for a LEO satellite in orbit, as it transits from minimum- to maximum elevation angle. An iterative method is implemented to calculate the parameters for the aircraft flight path, emulating the satellite elevation

Free space loss (dB)												
Altitude (km)	0.05	0.345	0.64	0.935	1.23	1.525	1.82	2.115	2.41	2.705	3	500
0 deg elevation	128.09	136.48	139.16	140.81	142	142.93	143.7	144.35	144.92	145.42	145.87	168.26
10 deg elevation	89.231	106	111.36	114.65	117.02	118.88	120.41	121.71	122.84	123.84	124.73	164.63
20 deg elevation	83.344	100.12	105.49	108.78	111.16	113.02	114.56	115.86	116.99	117.99	118.89	161.58
30 deg elevation	80.046	96.822	102.19	105.48	107.86	109.73	111.26	112.57	113.7	114.7	115.6	159.22
40 deg elevation	77.864	94.641	100.01	103.3	105.68	107.55	109.08	110.39	111.52	112.53	113.42	157.45
50 deg elevation	76.34	93.117	98.484	101.78	104.16	106.03	107.56	108.87	110	111	111.9	156.13
60 deg elevation	75.275	92.052	97.419	100.71	103.09	104.96	106.5	107.8	108.94	109.94	110.84	155.17
70 deg elevation	74.566	91.343	96.71	100	102.38	104.25	105.79	107.09	108.23	109.23	110.13	154.52
80 deg elevation	74.158	90.935	96.303	99.595	101.98	103.84	105.38	106.69	107.82	108.82	109.72	154.15
90 deg elevation	74.025	90.802	96.17	99.462	101.84	103.71	105.25	106.55	107.69	108.69	109.59	154.03

TABLE I
FREE SPACE LOSS CALCULATIONS

time window. An elevation time window is calculated for each combination of aircraft altitude and speed. It should be noted that if the altitude changes, so does the minimum distance to the ground station, which is the distance from the ground station to the satellite nadir point, when the aircraft is closest to the ground station.

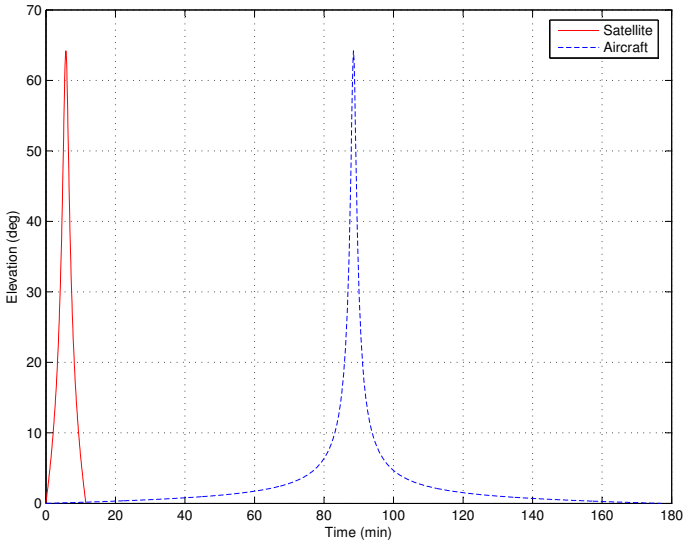

Fig. 4. Elevation angle versus time

Figure 4 compares the satellite and aircraft elevation angles versus time, for a chosen flight path. It is clear from Figure 4 that only a small interval of the visibility time period of an aircraft is suitable to emulate the behaviour of the time varying elevation angles of a satellite. For this reason the graph of the aircraft flight path is shifted to the left, to align the maximum elevation angles. The optimisation of the elevation time graph is achieved by calculating the area under each graph for a specified time window and subtracting the results. The smaller the result after the subtraction, the better the match between the two graphs. The results of these calculations are obtained from the script in the form of two figures. The dark blue areas in Figure 5 specify the areas where the speed and altitude of the aircraft best conform to the emulated elevation and azimuth angles. Figure 6 shows the distance for different altitudes from the aircraft's nadir point to the ground station at the point when the aircraft is closest to the ground station. Figures 5 and 6 enable us to choose either the desired speed, altitude or distance from the ground station and then use the figures to calculate the other parameters. Therefore, using the results from Figures 5 and 6, will allow us to specify the final flight route as required.

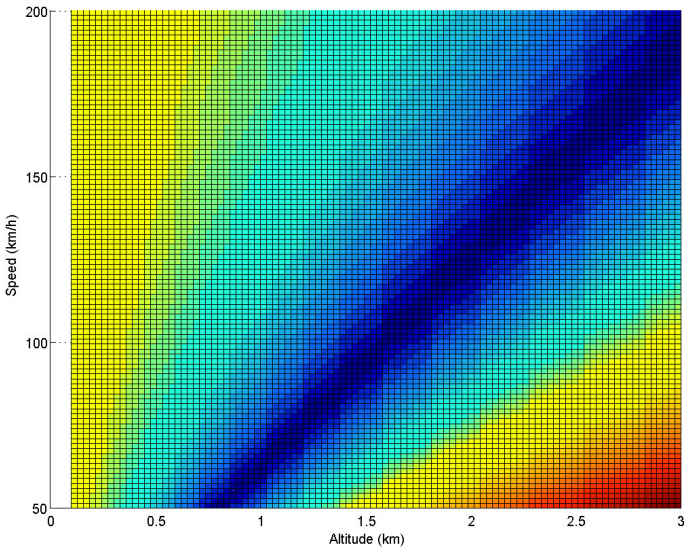

Fig. 5. Speed versus altitude of aircraft

It is thus possible to calculate aircraft flight path parameters of speed, altitude and distance from the ground station to satisfy the elevation and azimuth angles as related to the satellite's orbital flight. Figure 7 and Figure 8 illustrate this conformity between the elevation and azimuth angles of the satellite and the aircraft for the visibility time period of the satellite. Although deviations will occur at low elevation angles, a very useful time window for testing purposes can still be obtained.

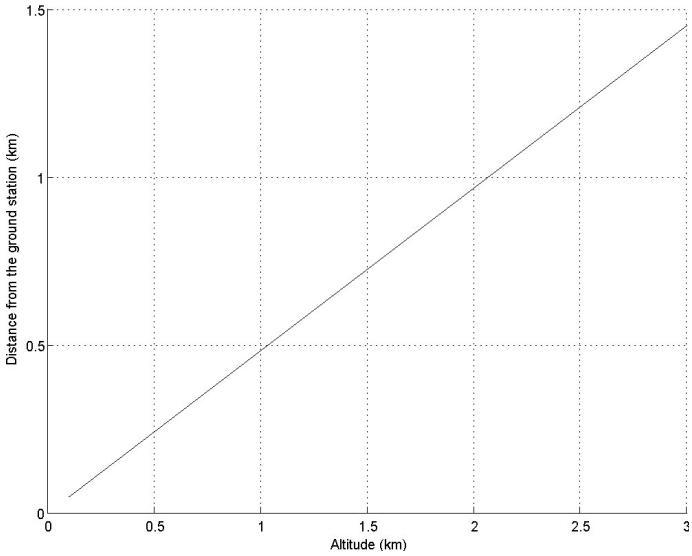

Fig. 6. Distance from ground station

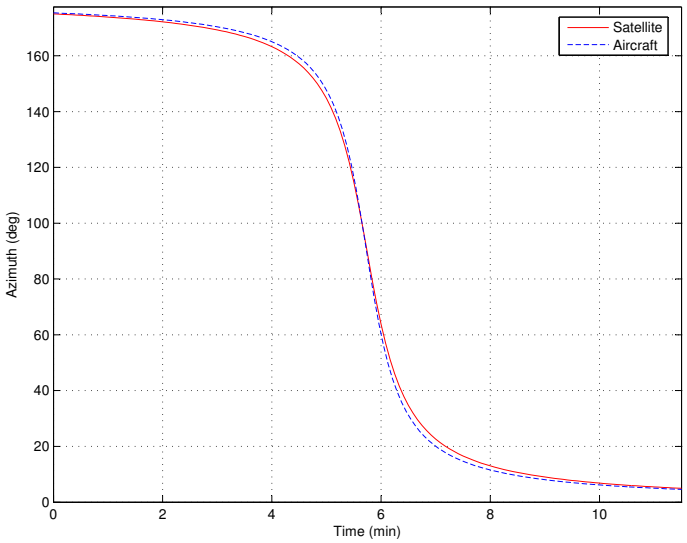

Fig. 8. Azimuth angle versus time interval

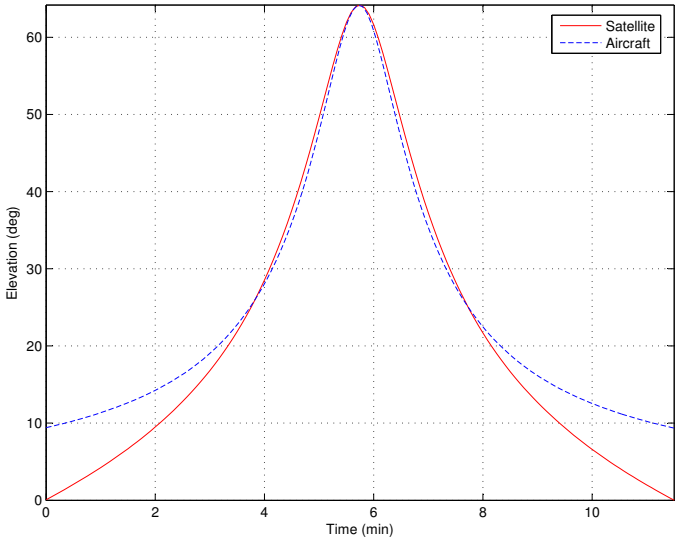

Fig. 7. Elevation angle versus time interval

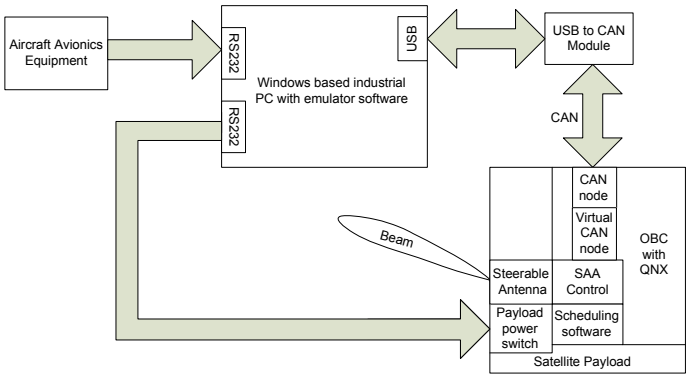

Fig. 9. System diagram

V. System Design

The system design is comprised of two sections, the emulator and the satellite payload modules. Only the components indicated in the system diagram as per Figure 9, have a direct influence on the system design. Components not directly affecting the system, are not shown.

A. Satellite Payload Module

The following components on the payload are applicable to the system design:

- Steerable antenna developed by KUL.
- The OBC, an SH4 processor with a 32-bit RISC architecture.
- A QNX operating system is run on the OBC. This UNIX based real-time operating system was provided by SunSpace, with additional software components.
- The scheduling module comprises software that schedules the communication times between the satellite and various ground stations.
- An SAA control module electronically controls the steerable antenna array. The required control algorithm was developed in the course of this project. The module uses the ϕ and θ steering angles to direct the antenna beam, according to the strategy to calculate these angles as discussed earlier. The SAA module is housed in the OBC of the payload.
- The CAN node, which allows devices to connect to the CAN network.
- A virtual CAN node enables the SAA control software to use the hardware of the exsisting CAN node on the OBC to communicate over the CAN bus.

B. Emulator Module

Instead of connecting the payload to a satellite through the CAN bus, the payload is connected to the emulator module, which mimics the behaviour of an actual satellite. The emulator module comprises an industrial PC with emulator software, known as the ASE, which provides an interface for the user to construct a flight path for an airborne object emulating the orbital characteristics of a satellite pass as closely as possible. As the emulation strategy is to fly the payload with the emulator module on an aircraft, the emulator module connects to the aircraft avionics equipment. Just as the satellite would provide data to the payload in flight, the emulator will provide the necessary data.

The aircraft satellite emulator design is divided into three sections, i.e., the aircraft avionics equipment interface, the ASE - payload interface and the satellite emulator software running on the industrial PC.

The ASE is connected to the aircraft avionics equipment via a RS232 port and to the payload CAN bus, via a USB to CAN module. The ASE software functions as implemented, can be summarised as follows:

1) One of the main tasks of the satellite emulator software, is to provide a GUI that will allow the user to construct a flight path for an aircraft to emulate a satellite, store flight data and display results. A GUI constructed flight path, with way points indicating the start- and end of the path, is shown in Figure 10. A GUI will allow a user to specify the ground station coordinates, maximum elevation angle and aircraft speed. The application will then calculate the speed, altitude and distance from the ground station required from the aircraft flight to satisfy the elevation and azimuth angles. The elevation and azimuth angles for the visibility time period as calculated, are displayed to the user, assisting with flight path definition.
2) The ASE software also calculates all the line-of-sight (LOS) link margins, elevation and azimuth angles of a satellite with specific parameters, for a specified amount of time.
3) The ASE software accepts the aircraft avionics inputs and does the necessary in-flight realtime translation to provide emulated data to the payload OBC via CAN bus. Flight data are recorded and used to calculate the aircraft LOS link margins, elevation and azimuth angles. The results of these calculations will be displayed to the user (typically an aircraft engineer/passenger), enabling him to to evaluate the flight continuously.
   The free space loss (FSL) parameter needs to be compensated for to emulate the satellite linkbudget. Figure 20 shows the calculated FSL over flight time. The aircraft link must thus be attenuated to obtain the correct satellite link FSL.
4) All the data received and sent by the ASE are logged by a script written in C. The SAA steering angles calculated by the control algorithm are also logged. This will enable the evaluation of the system performance after a flight. The SAA control can be thus be evaluated by perusing the logged data.
5) Close coordination was kept with the software developers of the OBC payload software, to ensure data/file compatibility and realtime data packet synchronisation between ASE and OBC/CAN bus.

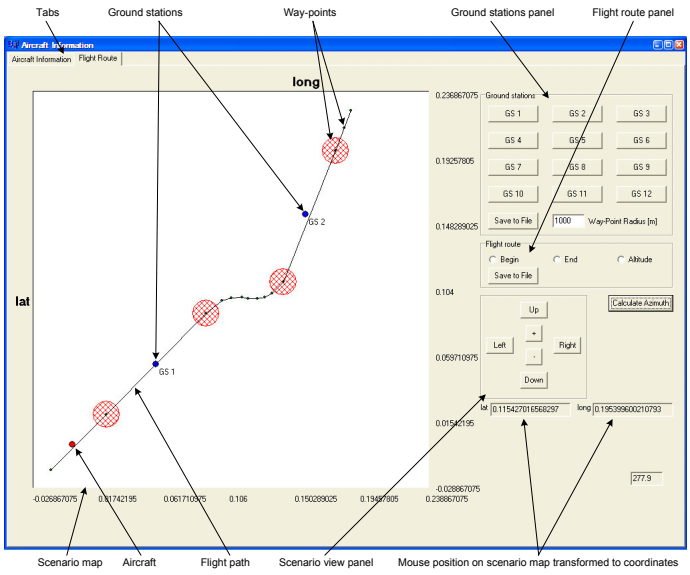

Fig. 10. Screenshot of the flight route tab of the GUI

C. Functional analysis

An understanding of the system can be achieved by discussing the various hardware and software modules, as per the system's functional block diagram of Figure 11.

D. Concept of Execution

1) Use Cases: All the entities that interact with this system and their corresponding use cases are shown in Figure 12. The emulation scenario is set up in the first use case. This is done by the user creating a flight route. A map with the flight route scenario is then displayed to the user. The second use case demonstrates the peripheral devices of the emulator being initialised by the user. These peripheral devices include the interface of ASE with the aircraft avionics equipment and the payload. In use case three data is received by the system from the aircraft avionics equipment. The data received describes the attitude and position of the aircraft. The system switches the payload "on" when the aircraft reaches the start of the flight route and "off" when the aircraft reaches the end of the flight route. This is illustrated by use case four, which simulates the situations as the satellite switches the payload "on" when communication with a ground station should start and "off" when communication ends. In use case five, QNX starts the execution of the antenna control software on board the SH4. This will occur each time the payload is switched on and the SH4 boots. In use case six the scheduling software

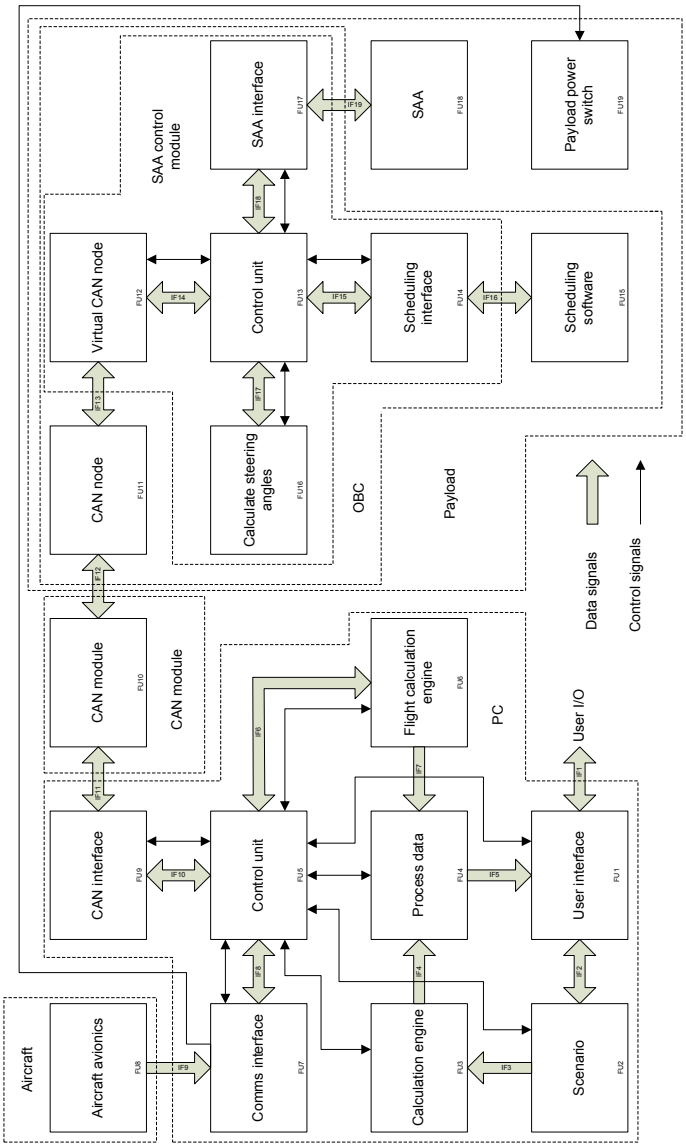

Fig. 11. Functional block diagram of the system

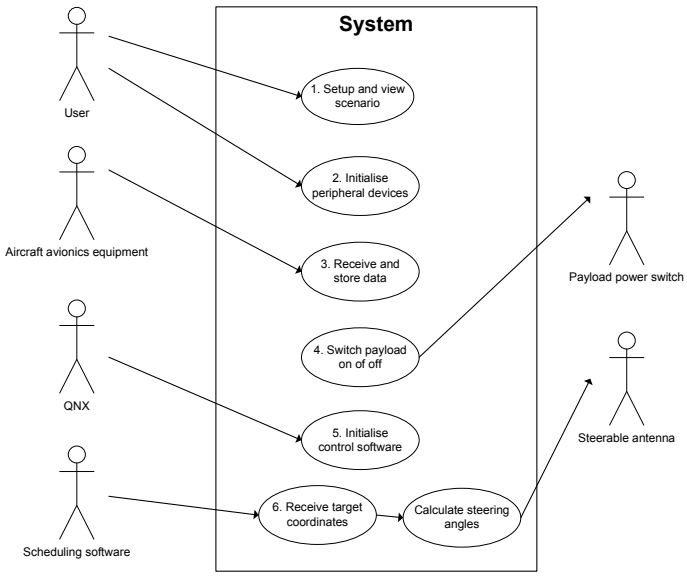

Fig. 12. System use case diagram

provides the coordinates of the target ground station to the system. The steering angles of the antenna are then calculated and the corresponding commands sent to the steerable antenna.

2) Sequencing: The sequential interaction of the various components defined by the use cases are illustrated by the sequence diagram of Figure 13. Note the following:

- The ASE continuously receives aircraft data from the aircraft avionics equipment.
- The ASE switches the payload on once the aircraft is at the start of the flight path. By switching the payload on, the steerable antenna will activate and QNX on the SH4 will boot. QNX will then start the execution of the scheduling and SAA control software. However, note that when the aircraft reaches the end of its flight path the ASE will switch the payload off. This will power down the steerable antenna, as well as QNX and the applications running on it.

E. Transmission Link

Subsection III-B describes the transmission link strategy adopted. The main concepts of this strategy are that:

- FSL should be compensated for to emulate the transmission link.
- The FSL compensation is achieved by attenuation of the received or transmitted signal.
- The attenuation will be applied at the ground station.
- For reasons mentioned in Section III-B, Doppler compensation is not considered. Doppler compensation will, however, be applied at the ground station when the system is implemented on an actual satellite.
- Flight tests will be performed in wide-open areas to minimise the effect of terrain scattering.

VI. Evaluation

In order to verify the design and subsequent usability of the system, some preliminary tests were performed to evaluate the emulator system performance before an actual flight test. The overall system performance was evaluated in four different ways, first with an aircraft avionics equipment emulator (AAEE), which was specifically developed for the evaluation of this system. The emulator serves as a substitute for an actual aircraft. Secondly, performance is evaluated with an aircraft simulator. The aircraft simulator closely models the light aircraft for which this system was developed. The aircraft simulator has input interfaces, such as a joystick and pedals, that contribute unknown factors such as pilot skill to the system evaluation. The third preliminary test used the aircraft simulator in conjunction with a prototype SAA to evaluate the system performance. The final ground based system test performed last, used actual aircraft telemetry data. This data

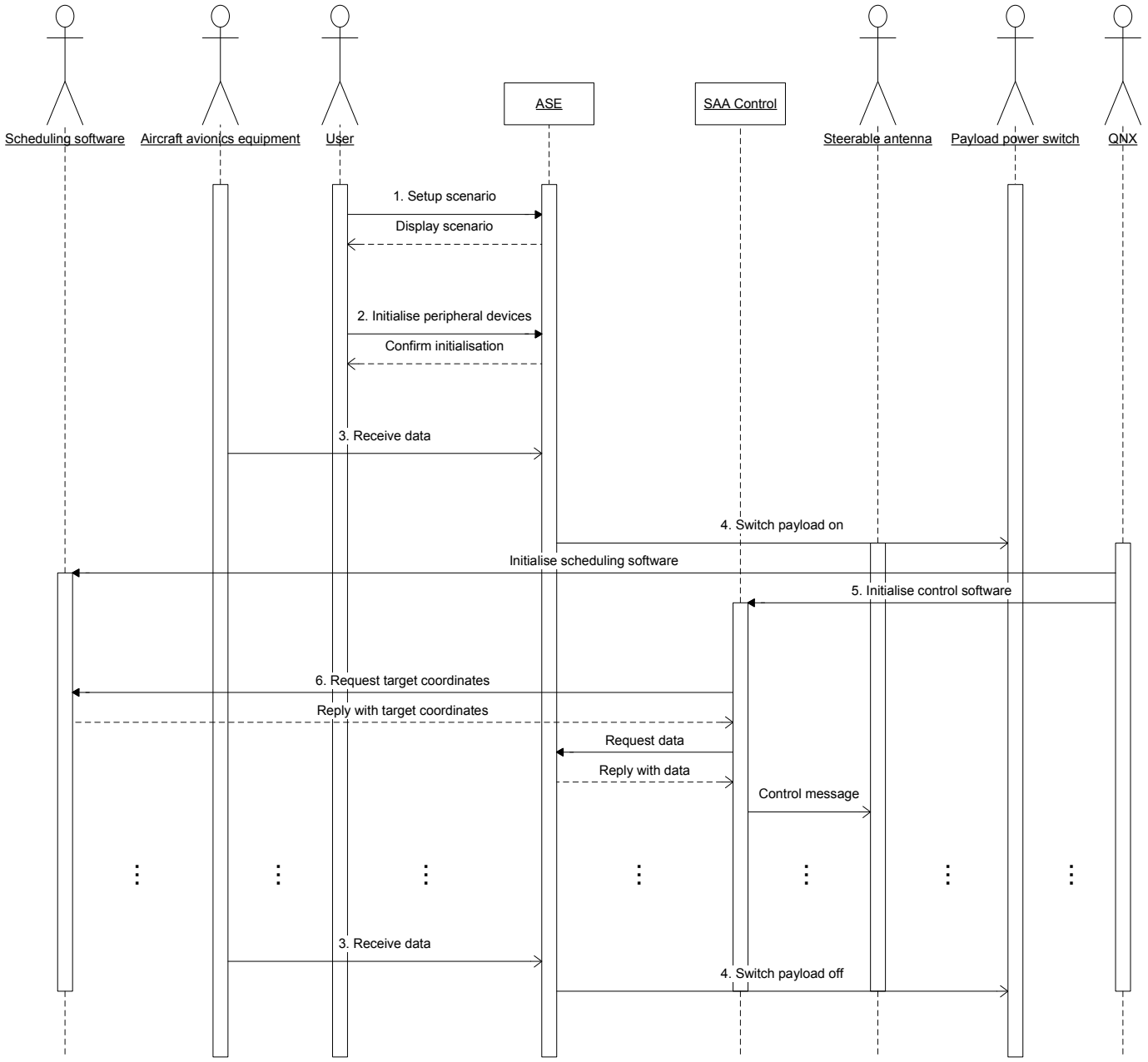

Fig. 13. System sequence diagram

was captured on a flight of the light aircraft for which this system has been developed. The tests were performed as follows:

1) During the course of the project, the AAEE software was specifically developed as part of the research. The software provides realistic aircraft avionics data with the correct protocol to the system, thereby providing a means to test the system without an actual flight test. The user can specify a chosen flight path by specifying the flight start-and-end coordinates as well as aircraft parameters such as velocity, altitude and attitude. The AAEE software uses this information to provide aircraft avionics data to simulate an aircraft flight.

As a first attempt, the AAEE was used to produce realistic avionics flight data, as for an envisaged test flight. This was run on a separate CPU and the data was serially fed into the ASE in real time. The ASE output, in reaction to the flight path as configured and simulated data as received, was fed onto the payload CAN bus for processing by the OBC. The latter was to produce the required steering commands for the SAA. The required steering angles, and commensurate commands, were calculated in advance using the orbital calculations as discussed earlier. The entire process was

logged by means of suitable scripts and the output of the payload to the SAA was captured on a separate PC.

2) As a second round of more stringent tests, approaching practical flight, a hardware based, standalone aircraft flight simulator was coupled to the ASE. The simulator is used for training and automatic pilot development. It is controlled by a joystick, pedals and other realistic hard interfaces, thus contributing the unknown quantity of pilot skill. Because the simulator closely models the light aircraft on which this system will be flown, the simulation will react in much the same way as the actual aircraft in flight. The simulator thus presents an extra dimension to the evaluation, without an actual flight test. Figure 14 shows a screen shot of the simulator GUI.

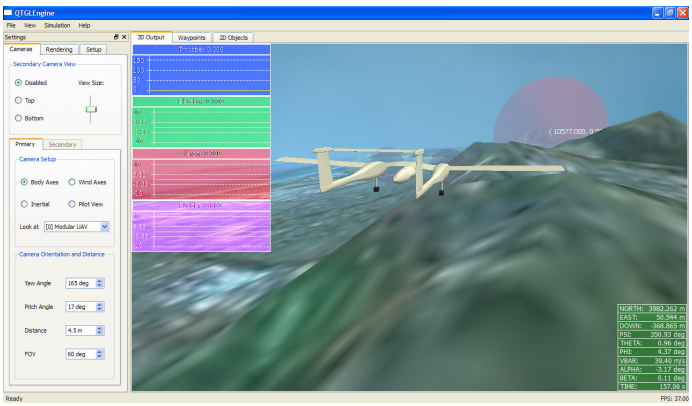

Fig. 14. Screen shot of the aircraft simulator software GUI

The ASE software was used to construct a flight route with a maximum elevation angle of $60°$. An above ground station altitude of $1.869\,\mathrm{km}$ is necessary for an aircraft cruising speed of $120\,\mathrm{km/h}$. As mentioned in Section III, the flight strategy would be to fly at a constant speed and altitude past a ground station, thereby emulating a LEO satellite pass. The results of this test are shown in Figures 15 to 20.

These figures present three sets of data. (For sake of clarity, some smaller portions of the graphs are magnified) The first two sets contain the predicted satellite and aircraft data. These were calculated with the help of calculations derived in Section II. The third set shows the aircraft flight data as generated by a simulated aircraft flight.

The attitude of the aircraft is described by Figure 15. The figure indicates the difficulty experienced in this case, in maintaining a constant attitude. It should be mentioned that the simulator was not flown on autopilot.

Figures 16 and 17 show the calculated elevation and azimuth angles. As can be seen from these two figures, the simulated flight data closely resembles that of the predicted aircraft flight. The elevation and azimuth angles are not that affected by the attitude, which is in line with the theoretical findings as presented earlier.

The calculated θ and ϕ angles are shown in Figures 18 and 19. A slight deviation is seen from the predicted aircraft data, which is attributed to the varying attitude of the aircraft. It is because of this expected deviation that the first approach mentioned in Section III was not chosen. A better approach is to emulate the elevation-azimuth angles more closely than the θ-ϕ angles, which will vary in any case. The antenna control algorithm uses these θ and ϕ angles to beam steer when the antenna steering control algorithm compensates for this varying attitude, as it should. The varying attitude should not affect the link budget significantly.

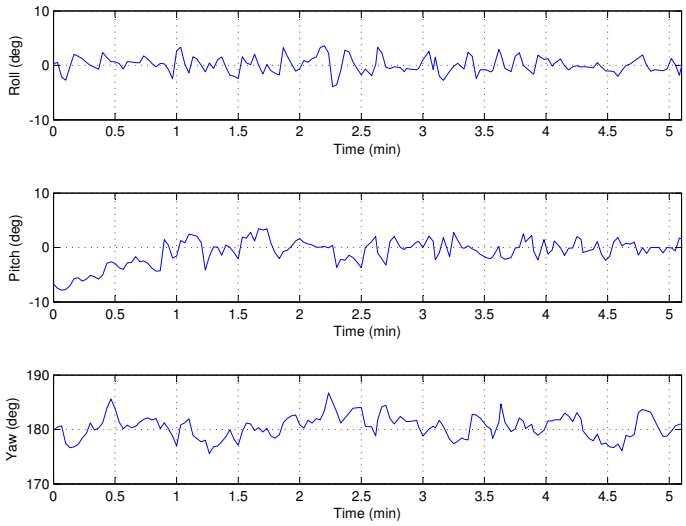

Fig. 15. Measured aircraft simulator flight test roll, pitch and yaw data

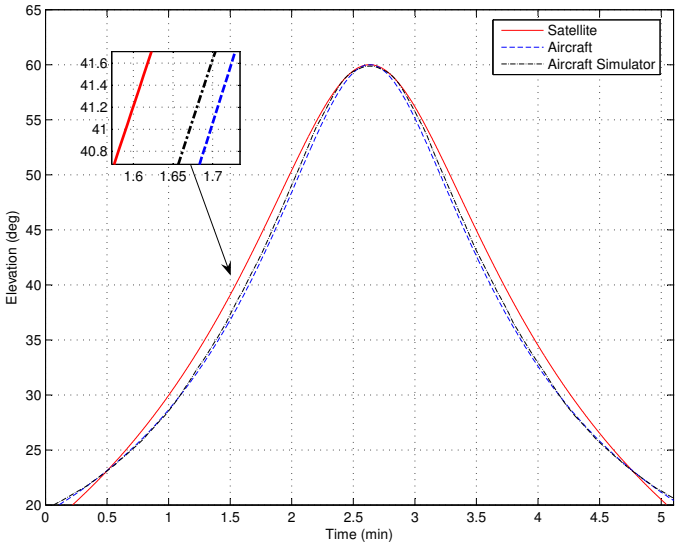

Fig. 16. Calculated satellite-, predicted aircraft- and measured aircraft simulator flight test elevation data

3) The following test was performed to evaluate the performance of the developed system with a prototype SAA, where the main focus was to see whether the two systems communicated correctly with each other. The

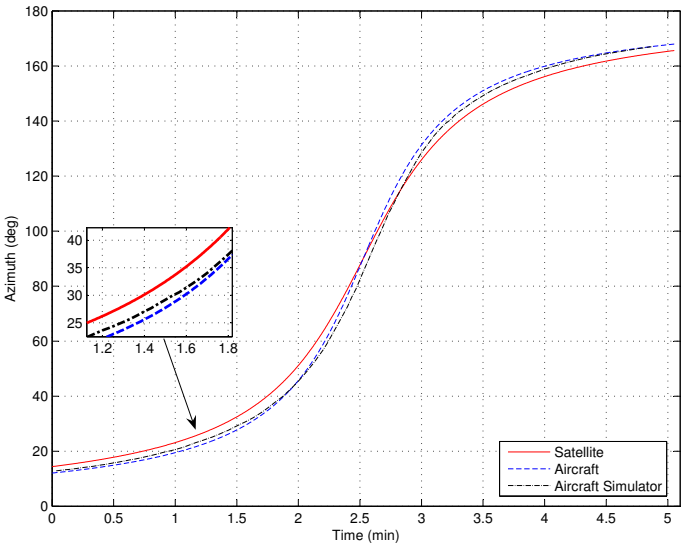

Fig. 17. Calculated satellite-, predicted aircraft- and measured aircraft simulator flight test azimuth data

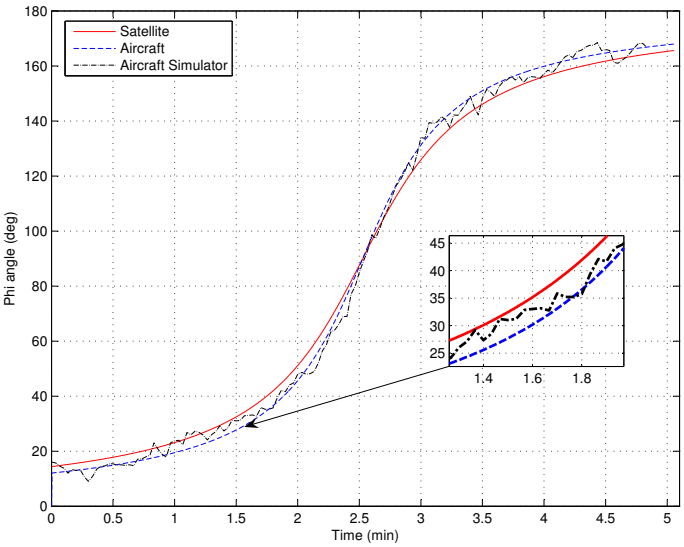

Fig. 19. Calculated satellite-, predicted aircraft- and measured aircraft simulator flight test ϕ angle data

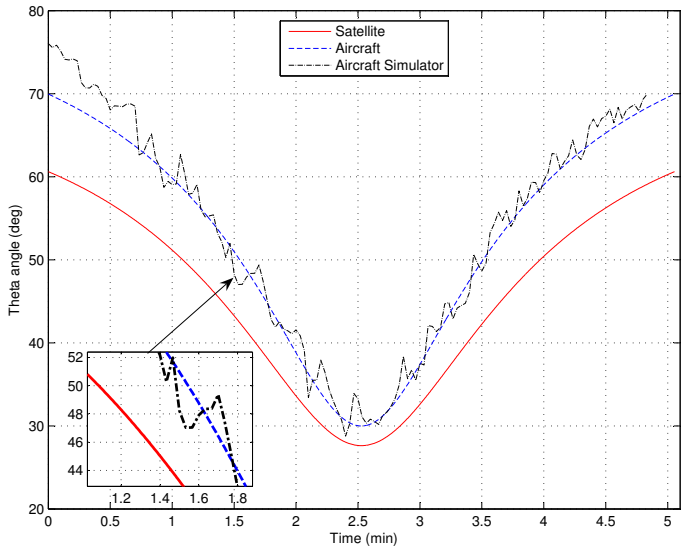

Fig. 18. Calculated satellite-, predicted aircraft- and measured aircraft simulator flight test θ angle data

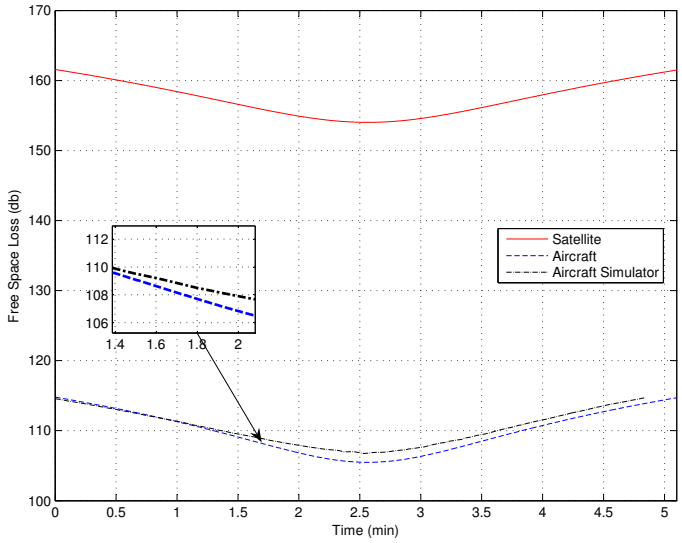

Fig. 20. Calculated satellite-, predicted aircraft- and flight simulator test FSL data

tests were performed in conjunction with KUL who, as mentioned earlier, developed the SAA.

The objective of the final test was first to confirm that the SAA control software on the payload can communicate with the SAA, then to verify that the SAA control software steers the SAA in the correct direction. To confirm the latter, the aircraft simulator was coupled to the system, a ground station was selected and the specified flight route flown.

A signal generator placed directly in front of the SAA provided a constant signal source to the SAA. A reduction of the received signal occurs when the SAA is steered. The SAA is steered according to the ASE indication of the aircraft on the flight route. Therefore, if the aircraft is directly above the ground station, no phase shift will be applied and the received signal will be at its strongest.

Data captured from the SAA confirmed that the SAA was indeed steered correctly. The SAA control module on the payload controlled the SAA as expected to enable the SAA to phase shift the signal correctly in order to direct the antenna beam to a specific ground station. KUL reviewed the data captured from the SAA and also concluded that the SAA was steered according to the specified flight path, confirming that communication between the payload and SAA was correct.

4) The final system test once more increased the level of realism, before an actual flight test. The system

test utilised captured telemetry data from a flight of the light aircraft test vehicle. Actual telemetry data introduces another unknown factor into the evaluation process, in the form of wind disturbances and other flight perturbations. The data generated by the system was captured and evaluated, as with the previous tests. The test proceeded as follows:

A flight path was first constructed with the help of the ASE software. The path past a ground station had a maximum elevation angle of $50°$, an altitude of $1.985\,\mathrm{km}$ above the ground station and required a cruising speed of $130\,\mathrm{km/h}$. The flight path was then flown with a light aircraft. The aircraft telemetry data was captured in flight and retrieved afterwards. Note however, that only half of the flight path constructed by the ASE, was flown. The reason for this is that the data for the second half of the flight path would be a mirror image of the first, which was therefore, considered adequate for these initial system tests. The light aircraft used for the flight, is depicted in Figure 21.

Fig. 21. The Jora flight test aircraft

The following four figures describe the telemetry data captured from the flight. The first set of data illustrated in Figure 22 shows the aircraft flight route as the aircraft flew in a North-Westerly direction past the ground station. Figure 23 shows the aircraft altitude above the ground station, Figure 24 the aircraft airspeed and Figure 25 the attitude. Note that Figure 24 illustrates the speed of the aircraft through the air and not the speed relative to the ground. Factors such as the wind needs to be taken into account when calculating the aircraft ground speed.

As depicted by the figures regarding the aircraft simulator based system test, these figures illustrate the difficulty experienced by the pilot in maintaining a constant heading, altitude, speed and attitude. These deviations can also partly be attributed to external factors such as wind disturbances. However, note that the attitude with these wind disturbances are more or less the same as the attitude obtained earlier with the aircraft simulator in Figure 15. These disturbances could possibly be minimised by an experienced pilot flying in a relatively calm day.

After the telemetry data was retrieved, the flight data was fed to the ground based system test setup. This setup is

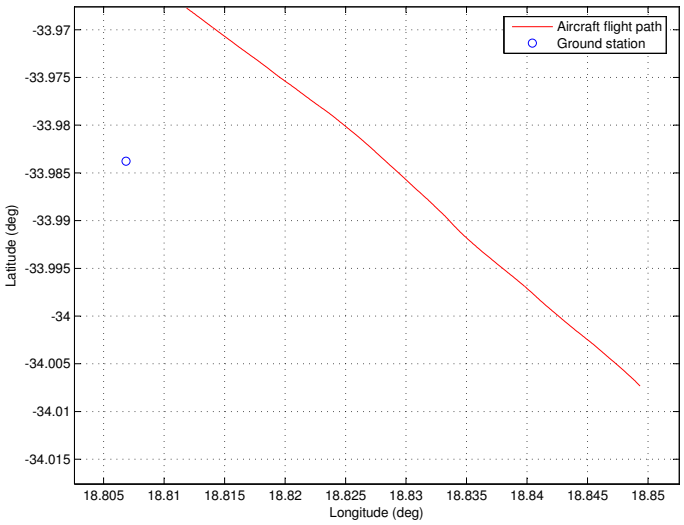

Fig. 22. Aircraft flight path past ground station

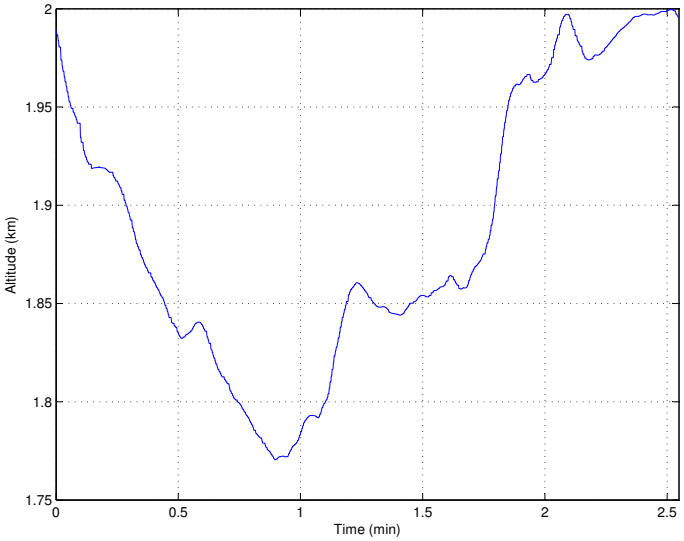

Fig. 23. Aircraft altitude above ground station

exactly the same as for the previous system tests, except that the input data is sourced from the actual aircraft flight telemetry record. The results of this test are shown in Figures 26 to 29.

The elevation and azimuth angles are shown in Figure 26 and 27. It is clear from these results that the actual elevation and azimuth angles closely follow the predicted values, as in the case using the aircraft simulator. This is in line with the results from previous system tests and a gratifying confirmation thereof.

Figure 28 and 29 shows the θ and ϕ steering angles. These angles are also in line with the results obtained by the earlier system test. Similar to the indications of the earlier test, small deviations from the predicted aircraft data can be seen, attributed to varying altitude, speed and attitude. This data however, also shows that these

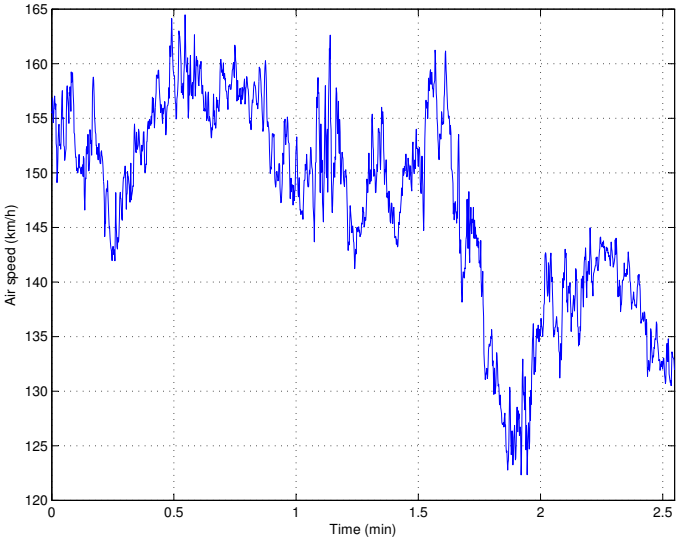

Fig. 24. Aircraft air speed

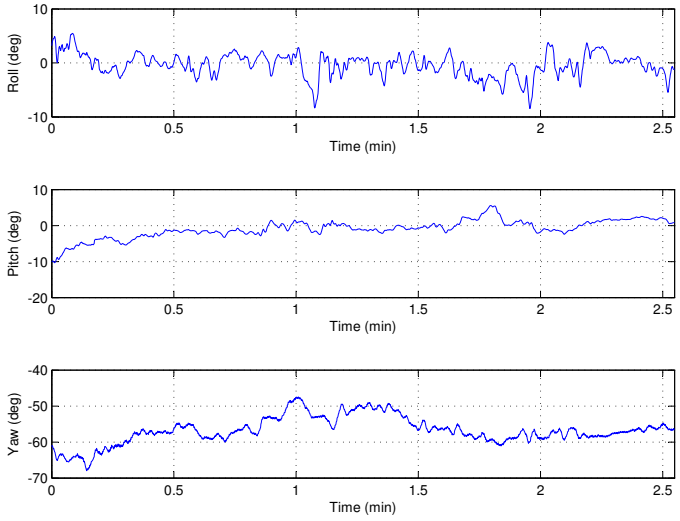

Fig. 25. Aircraft attitude

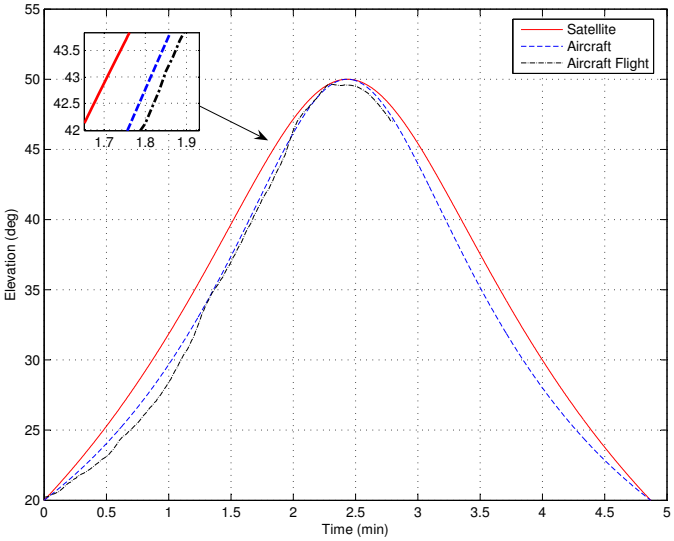

Fig. 26. Calculated satellite-, predicted aircraft- and measured aircraft flight test elevation data

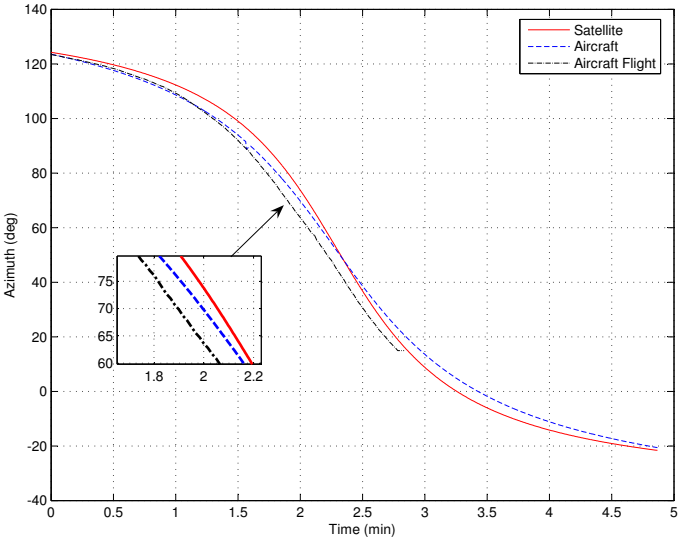

Fig. 27. Calculated satellite-, predicted aircraft- and measured aircraft flight test azimuth data

deviations are more or less the same as experienced with the earlier aircraft simulator based tests. It also serves to further confirm the soundness of concept using an appropriate aircraft based emulator as an interim test bed for this type of satellite system.

Figure 30 shows the calculated FSL. The losses resemble the predicted figures and the link budget will not be significantly affected by the aircraft attitude, due to the steerability of the antenna.

The tests as abovementioned, have proved the functionality of the design and no reason that the design should not perform as expected in the actual flight test, has been uncovered. The results obtained by using actual aircraft telemetry data confirmed those obtained previously with the aircraft simulator. At the time of of writing, an actual flight test with fully integrated system was scheduled for the second half of 2011. Equipment racks in the aircraft have already been prepared to receive the ASA, SAA and test platform hardware.

VII. Conclusion

The initial results obtained by means of an aircraft simulator and flight telemetry, confirm the requirement to follow an exact flight route while maintaining a constant attitude. Any deviation will affect the performance of the emulation. However, the elevation and azimuth angles are less affected than the θ and ϕ angles by small aircraft attitude fluctuations, for reason that the elevation and azimuth angles are measured from the perspective of the ground station and θ and ϕ from the aircraft.

Attitude changes obviously also change the orientation of

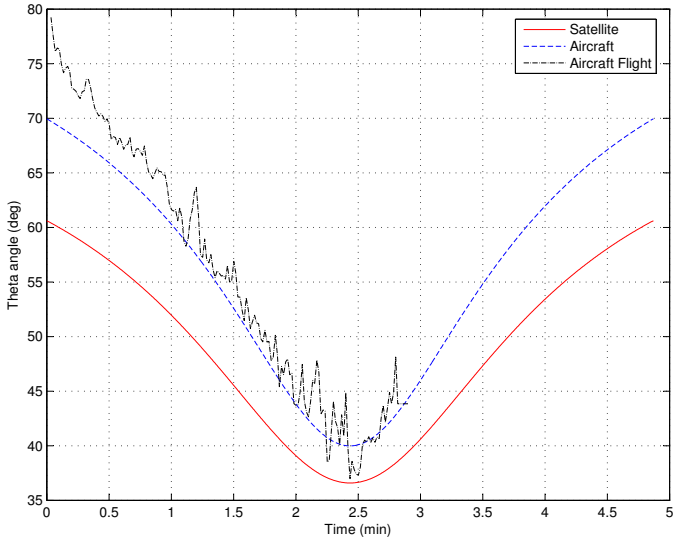

Fig. 28. Calculated satellite-, predicted aircraft- and measured aircraft flight test θ angle data

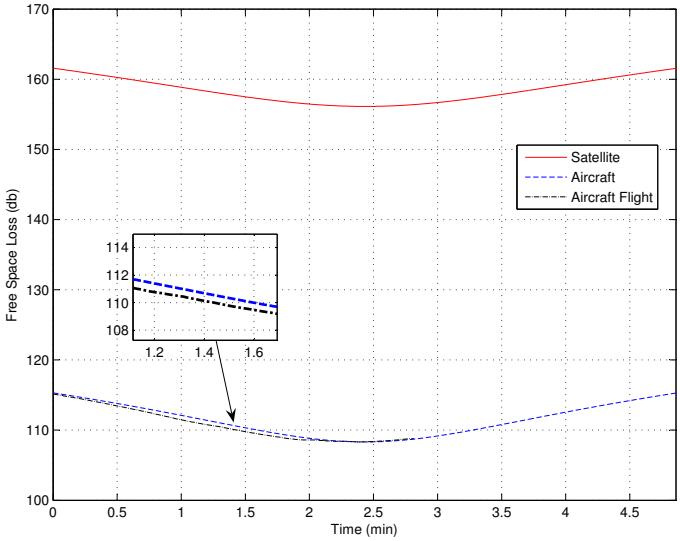

Fig. 30. Calculated satellite-, predicted aircraft- and flight test FSL data

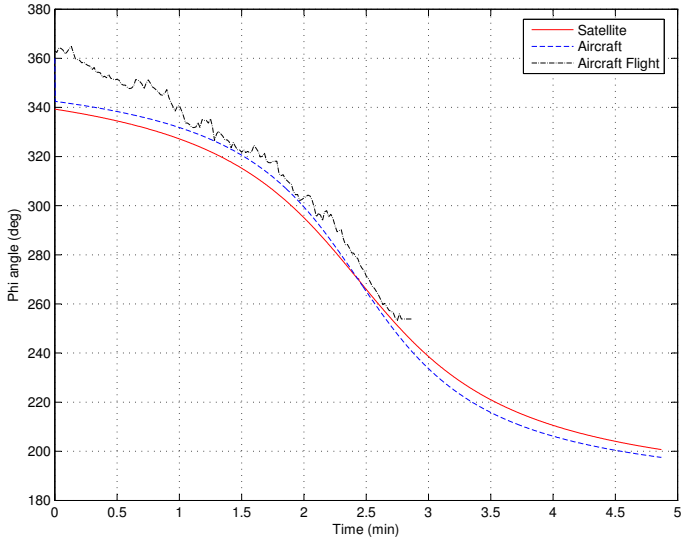

Fig. 29. Calculated satellite-, predicted aircraft- and measured aircraft flight test ϕ angle data

the antenna on the aircraft. This, however, will be compensated for by the antenna control algorithm in correcting the θ and ϕ steering angles (Figures 18, 28 and 19, 29). The effect on the transmission link is, therefore, relatively small, apart from some required change in the induced FSL (Figure 20).

Maintaining an exact flight path presented a challenge to the pilots flying the aircraft simulator and the actual light aircraft. An experienced pilot is essential for the successful implementation of the flight strategy. This was even more evident in the actual flight where external factors such as wind disturbances played a role. These external influences can be minimised by flying in good weather conditions and augmenting the flight operations with an autopilot.

Furthermore, results from the previous sections indicate that deviations occur at low elevation angles. A flight path with a higher maximum elevation angle will, therefore, emulate the satellite more accurately. This is not seen as a major drawback, as the emulation time window is still adequate.

Test logs from the performed tests also indicate that the beam steering commands were correctly generated by the OBC in response to the ASE inputs, in response to the ASE inputs as processed from the aircraft avionics parameters, flight path data as defined and ground station coordinates.

The initial results clearly indicate that it is quite feasible to use a light aircraft equipped with a suitable emulator, to act as an initial flight test platform, in order to evaluate the performance of the beam steerable satellite antenna and peripheral associated payload components. Although many other factors, such as overall hardware configuration, space endurance etc., enter into the design of actual space flight hardware, the economics and convenience of the approach as set out, are beyond question. It was also proved that an actual LEO satellite flight path could be emulated to an acceptable degree. The ASE with incumbent software as developed, will furthermore act as a realistic and flexible interface between the aircraft and the satellite payload under development. The set of results obtained thus far using actual hardware and very realistic flight data, confirmed the accuracy and functionality of the ASE. The tests performed with the prototype SAA further proved the functionality of the interface between the two systems and the correct operation of the OBC-SAA control software. This paper described the implementation and intermediate testing of a practical and quite general, LEO aircraft based emulation platform. This development is not only suitable for the SAA payload in question, but can be adapted for interim testing of various satellite payloads. Such an approach is a flexible and clearly cost effective means of actual preflight system testing. The system tests as documented stopped just short of full airborne equipment flight testing, as

scheduled for in the near future. However, as results up to the present have been very positive and in line with expectations, we look forward to that final step.

REFERENCES

[1] I. Kruger and R. Wolhuter, "An aircraft based emulation platform for LEO satellite antenna beam steering," in *Fifth International Conference on Systems and Networks Communication (ICSNC 2010)*. Nice, France: International Academy, Research, and Industry Association (IARIA), 22 - 27 August 2010, pp. 221 – 228.

[2] W. Aerts, P. Delmotte, and G. Vandenbosch, "Conceptual study of analog baseband beam forming: Design and measurement of an eight-by-eight phased array," *IEEE Transactions on Antennas and Propagation*, vol. 57, pp. 1667–1672, 2009.

[3] J. Wertz, Ed., *Spacecraft Attitude Determination and Control*. Kluwer Academic, 1991.

[4] D. Charlambous, "Mathematical tools (physics studies)," Department of Physics Lancaster University, Tech. Rep., page 4.

[5] B. A. Campbell and S. W. McCandless, *Introduction to Space Sciences and Spacecraft Applications*. Gulf Publishing Company, 1996.

[6] G. Maral and M. Bousquet, *Satellite Communications Systems*, 2nd ed. John Wiley & Sons Ltd, 1993.

[7] D. Koks, "Using rotations to build aerospace coordinate systems," Australian Department of Defence: Electronic Warface and Radar Division System Sciences Laboratory, Tech. Rep., 2006.

[8] "*Direction Cosine Matrix ECEF* to NED." [Online]. Available: http://www.mathworks.com/access/helpdesk/help/toolbox/aeroblks/directioncosinematrixeceftoned.html,(March2010)

[9] A. Thompson, "*Untitled Article*." [Online]. Available: http://atacolorado.com/eulersequences.doc(March2010)

[10] S. Cakaj, W. Keim, and K. Malaric, "Communications duration with low earth orbiting satellites," in *4th IASTED International Conference on Antennas, Radar and Wave Propagation*, Montreal, Canada, ARP 2007, May 30 - June 1 2007, pp. 85 – 88.